

# Cardiopulmonary Resuscitation Quality Parameters from Motion Capture Data using Differential Evolution Fitting of Sinusoids

Christian Lins<sup>a,b,\*</sup>, Daniel Eckhoff<sup>a</sup>, Andreas Klausen<sup>a</sup>, Sandra Hellmers<sup>a</sup>, Andreas Hein<sup>a,b</sup>,  
Sebastian Fudickar<sup>a</sup>

<sup>a</sup>*Carl von Ossietzky University Oldenburg, Dep. Health Services Research,  
Ammerländer Heerstr. 140, 26129 Oldenburg, Germany*

<sup>b</sup>*OFFIS - Institute for Information Technology, Div. Health,  
Escherweg 2, 26121 Oldenburg, Germany*

---

## Abstract

Cardiopulmonary resuscitation (CPR) is alongside with electrical defibrillation the most important treatment for sudden cardiac arrest, which affects thousands of individuals every year. In this paper, we present a robust sinusoid model that uses skeletal motion data from an RGB-D (Kinect) sensor and the Differential Evolution (DE) optimization algorithm to dynamically fit sinusoidal curves to derive frequency and depth parameters for cardiopulmonary resuscitation training. It is intended to be part of a robust and easy-to-use feedback system for CPR training, allowing its use for unsupervised training. The accuracy of this DE-based approach is evaluated in comparison with data recorded by a state-of-the-art training mannequin. We optimized the DE algorithm constants and have shown that with these optimized parameters the frequency of the CPR is recognized with a median error of  $\pm 2.55$  (2.4%) compressions per minute compared to the reference training mannequin.

**Keywords:** CPR training, cardiopulmonary resuscitation, curve fitting, differential evolution, cardiac massage, motion capture, sinusoid, Kinect

---

## 1. Introduction

In Europe, sudden cardiac arrests (SCA) is one of the most prominent diseases (350,000-700,000 individuals a year in Europe are affected, depending on the definition [1, 2, 3]) and can significantly affect the independent living of each individual if medical treatment is not available within few minutes [4, 5]. With medical treatment including ventilation, medication, and defibrillation

---

\*Corresponding author

Email address: christian.lins@offis.de (Christian Lins)

<sup>1</sup>This paper is an extended, improved version of the paper *Determining Cardiopulmonary Resuscitation Parameters with Differential Evolution Optimization of Sinusoidal Curves* presented at AI4Health 2018 workshop and published in: BIOSTEC 2018, Proceedings of the 11th International Joint Conference on Biomedical Engineering Systems and Technologies, Volume 5: HEALTHINF, Funchal, Madeira, Portugal, 19-21 January, 2018, pp. 665-670, ISBN: 978-989-758-281-3, INSTICC, 2018.

(Advanced Life Support, ALS) [6] there is a high probability of maintaining sufficient circulation thus a higher probability of surviving the incident. Medical personnel (including paramedics) is trained in ALS, but is usually not immediately available if a cardiac arrest occurs in the field. The typical median response time of paramedics is about 5-8 min [4], which is often too long to exclude long-term effects if no bystander (i.e. layman) CPR meanwhile took place. Immediate help is crucial because the functionality of the cells of the nervous system, including the brain, is reduced after 10 seconds (i.e. loss of consciousness) and the death of the cells begins after about 3 minutes [7]. Victims are therefore dependent on the help of bystanders. Thus, as the first minutes (golden minutes) after a cardiac arrest are the most important ones (the likelihood of survival decreases with every minute without CPR [8]), it is crucial that bystanders be well trained to provide appropriate help to the victim.

In case of a cardiac arrest, the most critical countermeasure is the cardiac massage (chest compressions) ideally in combination with rescue breathing (Basic Life Support, BLS) [4] to sustain a minimal circulation to carry oxygen to the nerve cells. During a cardiac massage, the heart is compressed by orthogonal pressure onto the breastbone. The depth of this compression is ideally 5 cm [4] to fully eject the blood from the heart. A complete decompression is crucial to fill the heart with blood again. The recommended frequency of the cardiac massage is 100 to 120 compressions per minute (cpm) [4]. If a sufficient rescue breathing parallel to the heart massage is not possible, i.e. if the victim is not intubated, the heart pressure massage will be briefly stopped and will be continued after two accelerated breathings (Figure 1 summarizes the BLS algorithm).

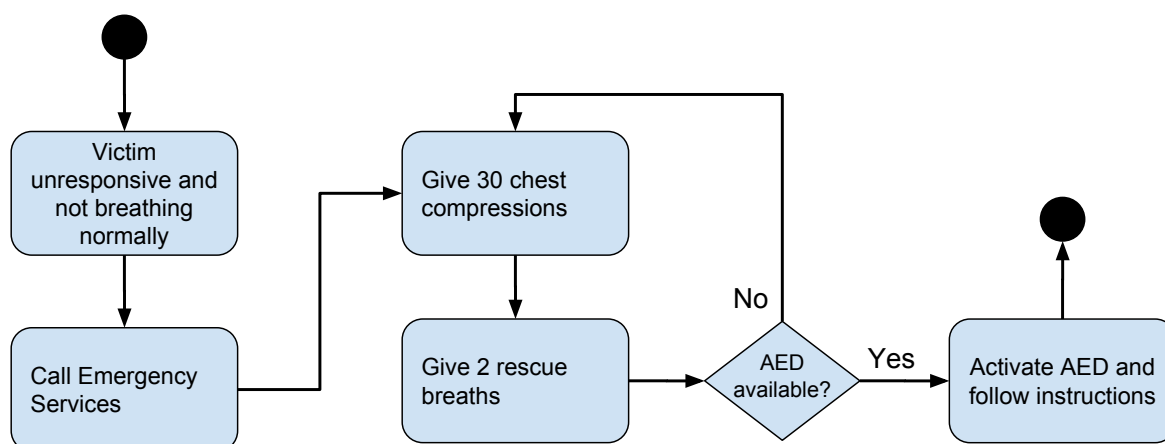


Figure 1: Flow diagram of the Basic Life Support algorithm [4].

High-quality CPR is significant to improve the outcomes of cardiac arrest, so proper training of medical personnel is as essential as the training of non-specialists, which can offer resuscitation support much faster [8]. Since ALS resuscitation training, due to the high material and training costs, is mainly used for medical professionals only, technological training systems might represent a well-suited alternative to train both professionals and non-specialists. Especially rural areas without proper training facilities could profit from feasible, low-cost training technologies. CPR can be trained with simulation mannequins, which typically provide real-time feedback of the

quality of cardiac massage and ventilation. Although the simulation mannequins provide immediate and precise feedback, they are limited to training situations. Under real conditions with human casualties, other techniques and technologies are needed to assist laypeople in CPR. A training mannequin with integrated pressure sensors is unsuitable for this. External sensors and devices could be an essential help along with audible and visual feedback. A widely used technology is the Automated External Defibrillators (AED), which are used to restore the regular heartbeat in the event of ventricular tachycardia (VT) or ventricular fibrillation (VF) employing an electrical shock. AED complements the ongoing (and still necessary) CPR. For example, an AED device might be equipped with optical sensors that allow it to capture a large part of the scene. Suitable algorithms are necessary for the evaluation of the visual observation of the resuscitation.

An approach with a low-cost RGB-D (RGB + Depth) camera such as the Microsoft Kinect (or even an RGB camera with software skeleton tracking) would provide a suitable alternative to regularly train larger audiences thus improving the overall quality of the CPR. As discussed, the CPR training with a system that incorporates external sensors holds advantages over the mannequin training. While mannequins can only provide accurate feedback regarding the compression frequency and depth as acquired by the integrated pressure sensors or IMUs, they can not detect the relevant space around and at the patient. They are therefore unable to give feedback regarding its posture of back and arms which have considerable influence on the endurance of the performed CPR and, thus are as well to be considered. Bystanders performing CPR with an ineffective posture will exhaust rapidly although their CPR frequency and compressions may be appropriate at the beginning. Only an (optical) motion capture (MoCap) system can provide such feedback on the posture. Besides, a motion capture based system may give feedback on the whole process of the ALS in professional training [6], e.g. regarding placing of tools, as well as regarding coordination and cooperation with the CPR partner.

Two crucial parameters of the CPR are the *frequency* at which the compressions are performed and the compression *depth* of the chest. Typically, the frequency is stated as compressions per minute (cpm) and the compression depth in cm. In this paper, we focus on these two parameters and propose a method to derive these parameters from motion data coming from an RGB-D-based skeleton tracking (Microsoft Kinect v2). We utilize the periodic nature of the CPR and use the time series distances of upper limbs to the floor to fit a sine curve (sinusoid) model so that we can robustly derive the two parameters mentioned above (see Figure 5).

With the proposed approach to monitor CPR execution with external Kinect sensors, CPR quality parameters such as the compression frequency and the compression depth can be derived without simulation mannequins. Thereby, the discussed disadvantages associated with mannequins are overcome and instead, the system is suitable for CPR training or in-situ observations, e.g. in a shock room.

RGB-D cameras have already been used in different approaches to support CPR training. Tian et al. for example use Kinect data to model a virtual environment with patient and trainee and drive a haptic device in the real world [9]. In the virtual environment, the performer can see the CPR on a virtual avatar while responding to the sensation of the haptic device. The authors focus more on the basics of cardiac massage than specific optimization of the training.

Semeraror et al. and Loconsole et al. present results from their system called RELIVE which is similar to our approach [10, 11]. RELIVE uses data from the Kinect v1 and extract depth

and frequency parameters from the motion data with the intention to improve the quality of CPR (training). In contrast to our approach they use the raw RGB pixel and depth image data of the Kinect to identify hands, arms and the training body. The predecessor to RELIVE is probably the Mini-VREM tool, which is a Kinect with software-based audio- and video-feedback-system [12] but requires a marker at the subject's hands (colored bracelet).

Higashi et al. developed and evaluated an augmented reality system that enables the user to correct her or his posture while performing cardiac massage compression [13]. The focus of this work lays on the correct posture of the performer primarily to differentiate between extended position compression and bent position compression. Unfortunately, they have not yet provided a quantitative evaluation of their system.

Wang et al. have proposed a real-time feedback system for CPR training, using the *Kinect v1* sensor [14]. The system shows the current compression depth and frequency on a computer screen so that the trainee can adapt her or his actions accordingly. By evaluating the system with 100 healthcare professionals, the authors have shown that the system has significant effects on the CPR quality. Wang et al. system requires marker on the trainee's hand and the chest of the training mannequin. Additionally, the placement of the Kinect must be carefully chosen here as they directly derive the compression depth from the sensor data.

Our approach relies on the integrated skeleton tracking of the Kinect (other pose detection methods, e.g. OpenPose [15], might be feasible as well) and requires no individual markers nor prior calibration. Our method does not directly use the sensor data but fits it to a harmonic sine curve (sinusoid) to make the method robust against sensor noise or false recognition of the skeleton tracking. However, our approach requires a viable curve fitting algorithm.

To our best knowledge, no one has tried to fit the motion capture (MoCap) data of CPR training to a sinusoid, but there are several possibilities to fit the time series data to a (harmonic) curve. There are approaches described in signal processing literature to determine the frequency of noisy data. Zero crossing is a method that measures the time between two zero crossings of the signal, which is an indication for the frequency of the signal [16]. The Fourier decomposition [17, 18] or a Kalman-Filter [19] is also mentioned. Other methods are a recursive Newton-type algorithm [20] and adaptive notch filters [21]. Sachdev and Giray [22] used Taylor series and least-squares fitting to determine the frequency of a power system. The approach presented in this paper does not require Taylor series decomposition of a harmonic function but directly fits a sine curve. For this least-squares fitting, a minimization algorithm is needed. Differential Evolution (DE) [23, 24] is a heuristic search algorithm well suited for nonlinear functions. It is used for a wide range of applications, e.g. to extract parameters of solar power modules [25], to find solutions for the equation of Electro Hydraulic Servo Systems [26], or to fit bezier curves [27]. We show how the Differential Evolution optimization algorithm can be used to fit a sine curve which robustly provides the two wanted parameters. The DE algorithm is confronted with some constraints. First, the application must be running in real time to give feedback to the user. This requires a tradeoff between responsiveness and algorithmic runtime. Thus it is necessary to minimize the run time while sustaining sufficient precision. Moreover, second, the frequency and depth of the CPR are (in most cases) changing continuously, so the model, i.e. the sinusoid, must be adapted continuously as well.

To summarize our contributions:

- We present a practical and widely usable approach to facilitate skeletal motion capture data to derive two quality parameters (compression frequency and compression depth) of the CPR process using a fitted sinusoid model.
- We compared the suitability of wrists, hands, elbows, and shoulders to find out which limbs are best for determining CPR quality parameters when using skeletal motion capture. We show which influence the number of individuals and the window size  $S_{len}$  has on the model precision.
- We optimized the constants of the DE algorithm to efficiently fit the limb-floor-distances of the motion capture data to the sinusoid model to increase the efficiency of the approach.
- We evaluated our approach using 19 participants.

The outline of the paper is as follows: In Section 2 we present our approach in detail (2.1), explain the Differential Evolution algorithm (2.3), and outline the evaluation study (2.4). Section 3 contains the experimental result, which we discuss in Section 4. The paper is concluded in Section 5.

## 2. Materials and Methods

### 2.1. System Design

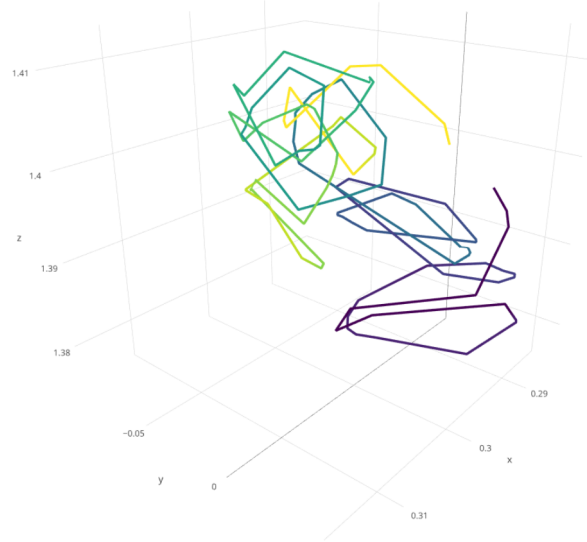


Figure 2: 3D visualization of shoulder joint coordinates while performing chest compressions.

An optical MoCap system can observe the full spatial spectrum, i.e. a 3-dimensional representation of the scenery. In our approach (see Figure 3), an optical MoCap system observes the scenery with a resuscitation in progress. The trainee sits at the side of a mannequin (here a simple sensorfree

plastic mannequin or another compressible object can be used) and performs thorax compressions. Figure 2 shows an exemplary 3D motion of one joint while performing thorax compressions. Because of the complexity of 3D motions we calculate the distance of upper limbs to floor, which effectively reduces the complexity. The resulting distances are fitted to a sine curve. The system recognizes the performance through the derived CPR quality parameters of the trainee and gives feedback.

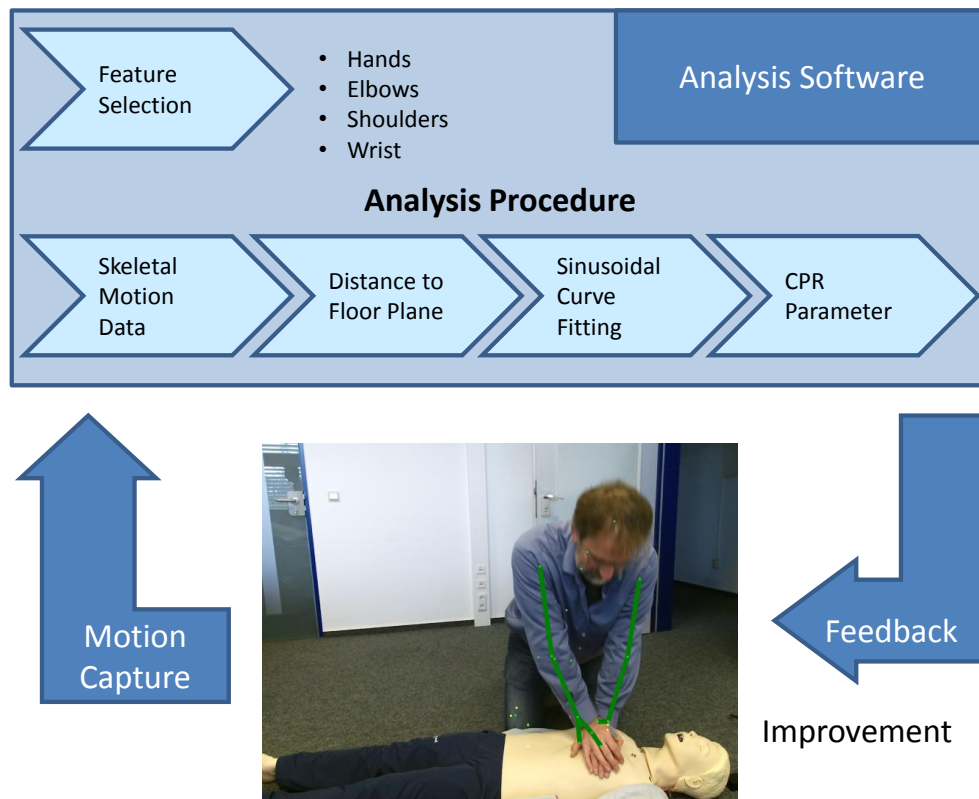


Figure 3: CPR training and feedback with Kinect

## 2.2. Implementation

We implemented the Differential Evolution algorithm and the visualization software using C# on a Windows system. Figure 4 shows a typical screenshot of the application while processing motion data from the Kinect sensor. The RGB image is shown on the screen together with a green line overlay representing the arms. Additionally detected skeleton joints are marked as small yellow dots.

The Kinect sensor API notifies our application when a new data frame is available from the sensor (Event-driven) and provides the application with a Skeleton frame containing the joint positions and the floor plane estimation. The application calculates the distance between the floor

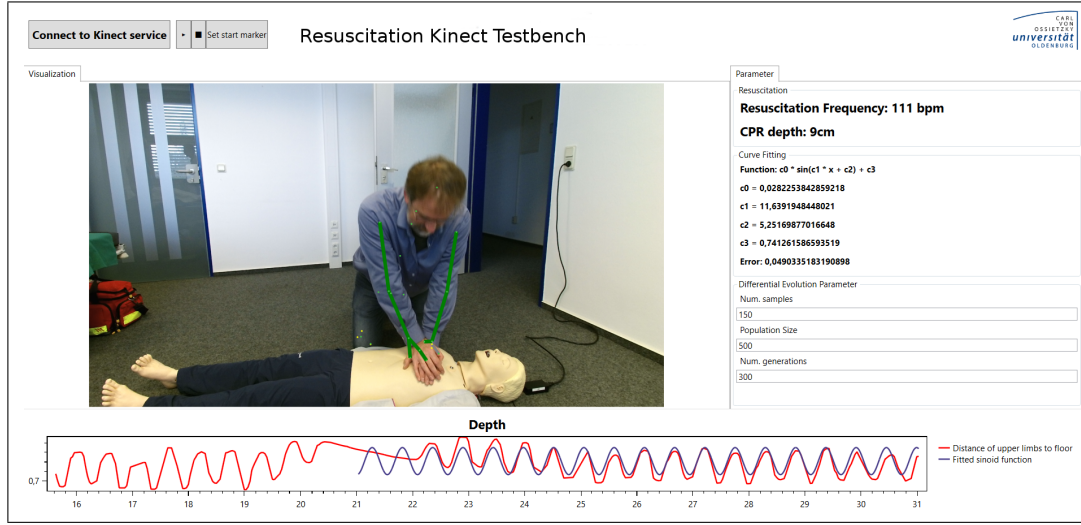


Figure 4: Our software RESKIN processing Kinect motion data from a CPR training session. The graph at the bottom shows the distances between the floor and the limbs (red) and the fitted sinusoid curve (blue).

plane and the upper limb joints. On every few samples (depending on the hardware performance and the current fitting error) the last  $S_{len}$  samples are being evaluated against the currently fitted sinusoid, and the Root Mean Square Error (RMSE) is calculated (see Section 2.3 for more details). The application continuously draws the current fitting in the graph on the bottom (see Figure 4).

### 2.3. Differential Evolution for Fitting Sinusoidal Curves

In this approach, a set of MoCap measurements is used to fit a sinusoid. The MoCap data consists of pairs (left and right) of 3D coordinates  $v$  over time  $t$ . The floor plane equation  $P_{Floor}$  can be derived from the Kinect sensor's floor plane estimation.

$$P_{Floor} : n_1 \cdot x + n_2 \cdot y + n_3 \cdot z = a \quad (1)$$

With the floor equation the distance  $d(t)$  from floor to joint can be calculated for every measurement sample:

$$v(t) = \frac{v_{Left}(t) + v_{Right}(t)}{2} \quad (2)$$

Be  $v(t)_x, v(t)_y, v(t)_z$  the three components of the 3D vector  $v(t)$ .

$$d(t) = \frac{n_1 \cdot v(t)_x + n_2 \cdot v(t)_y + n_3 \cdot v(t)_z - a}{\sqrt{(n_1)^2 + (n_2)^2 + (n_3)^2}} \quad (3)$$

A set of this samples  $d(t)$  forms a sample set  $S$ :

$$S = (d(t), \dots, d(t - S_{len})) \quad (4)$$

The value of  $S_{len}$  is to be determined.

### 2.3.1. Minimization Problem

Our approach utilizes the periodic nature of the CPR to fit the time series of distances (upper limbs to ground) to a sine curve (see Figure 5).

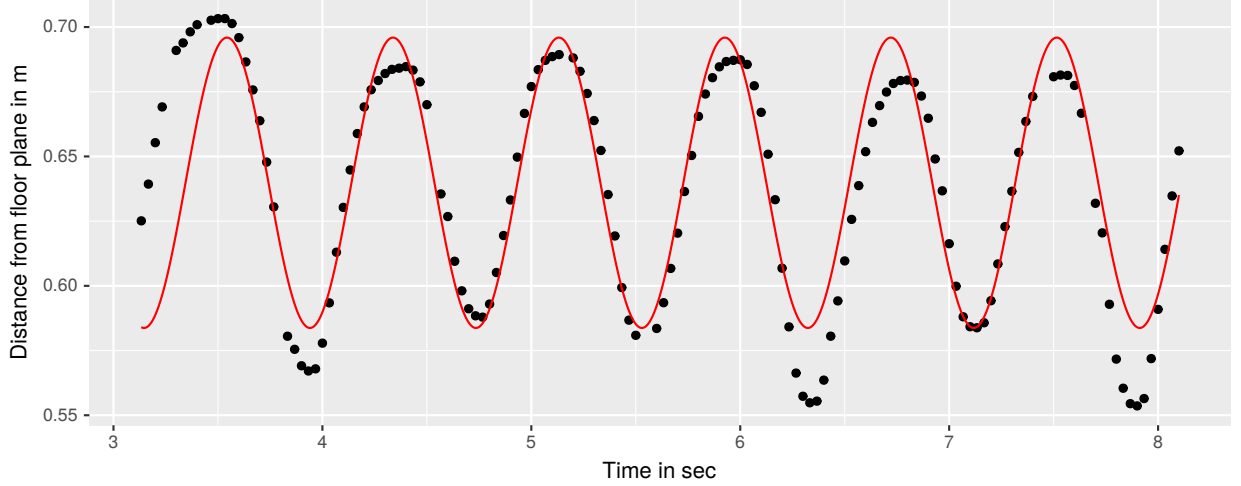


Figure 5: Fitting a sinoid to Kinect distance data. In this excerpt from actual evaluation data, a data segment of  $S_{len} = 5$  seconds was used.

The generic sine function with four parameters can be written as follows:

$$y(t) = A \cdot \sin(2\pi ft + \rho) + D \quad (5)$$

As parameters, the amplitude  $A$  and the ordinary frequency  $f$  are of primary interest here. When assuming that the arms of a person performing CPR are orthogonal (and rigid) on the patient's chest, then the relative distances of his/her arms are equal to the chest compression depth. Moreover, the frequency of low to high to low compression depth represents one compression cycle. To find a robust CPR frequency and compression depth, we fit the time-series data of upper-limb distances to a sinusoidal curve. On a fitted function, parameter  $f$  is the CPR frequency and  $A$  is the compression depth. Parameter  $D$  shifts the function values in Y-direction and  $\rho$  represents the phase shift.

To fit the function  $y(t)$ , we minimize the cost function (here: RMSE) using an evolutionary approach.

We can formulate this as a minimization problem:

$$\min \sqrt{\frac{1}{|S|} \sum_{t=0}^{|S|} (S(t) - y(t))^2} \quad (6)$$

with  $S$  being a  $S_{len}$ -length vector of joint-floor-distances  $d(t)$  (see Equation 3).



### 2.3.2. Differential Evolution

The Differential Evolution algorithm [23] is a generic evolutionary optimization algorithm that works particularly well with nonlinear, i.e., sinusoidal cost functions. DE searches and evaluates a parameter space concurrently and finds multiple near-optimal but distinct solutions to a problem.

As all evolutionary algorithms, DE is population-based and optimizes the individuals of the population (sometimes called agents) throughout several generations:

$$x_{i,G} \text{ with } i = 1..NP, G = 1..G_{max} \quad (7)$$

$x_{i,G}$  is a 4-dimensional vector (because of the four unknowns of Equation 5) of individual  $i$  for generation  $G$  representing one possible solution to our problem (see Equation 6). So in every generation,  $NP$  individuals are optimized up to  $G_{max}$  generations.

The optimization is done between a transition from one generation  $G$  to another generation  $G + 1$ . Most evolutionary algorithms – as does DE – comprise the steps mutation, crossover, and selection, which are discussed in the following subsections. Each of these steps influences the convergence and runtime characteristics of the algorithm.

*Mutation.* For every generation, a mutation step is performed for every individual  $x_{i,G}$ . We used the step from [23] with a (at first) fixed amplification factor  $F$ :

$$v_{i,G+1} = x_{r_1,G} + F \cdot (x_{r_2,G} - x_{r_3,G}) \quad (8)$$

with  $v$  the mutated individual and  $r_1, r_2, r_3 \in \{1, 2, \dots, NP\}, r_1 \neq r_2 \neq r_3 \neq i$  randomly chosen. The strategy in Equation 8 is labeled as DE/rand/1/bin, which is the original mutation strategy from [23]. There are a few other mutation strategies that lead to different convergence behavior (see Table 4).

*Crossover.* The crossover step decides which of the four parameters of one individual are preserved in the next generation. For every parameter a uniform random number  $r \in [0, 1]$  is chosen. If  $r \leq CR$  then the parameter from the mutant is chosen, otherwise the one from the original individual.

*Selection.* The selection step decides which individual is passed to next generation by evaluating it against the cost function. In our approach the RMSE is summed up for every solution candidate  $x_{i,G}$ :

$$c_{x_{i,G}} = \sum_{t=0}^T (S(t) - y_{x_{i,G}}(t))^2 \quad (9)$$

with  $S$  being a  $T$ -length vector of samples (joint-floor-distances) and  $y$  the parameterized sinusoid function (Equation 5) of individual  $x_{i,G}$ . If  $c_{v_{i,G+1}} < c_{x_{i,G}}$  the mutated individual  $v$  is passed to the next generation otherwise  $x$ .

## 2.4. Study Design

We have previously confirmed the general suitability of the application of Differential Evolution algorithm to optimize the sinusoid curve describing the CPR parameters compression frequency and compression depth [28]. For this evaluation, we investigated which of the upper limbs/joints, i.e. wrists, hands, elbows, or shoulders, are most suitable for the determination of CPR parameters (Feature Selection, see Figure 6). Additionally, we examined different values for the number of individuals  $NP$  and the ideal sample set length  $S_{len}$ . After choosing an optimal  $NP, S_{len}$ , we probed every mutation strategy and optimized the DE parameters  $F$  and  $CR$  to improve the convergence specific to the domain further, thus minimizing the required computing power to retrieve a satisfactory result (Step 2, see Figure 6).

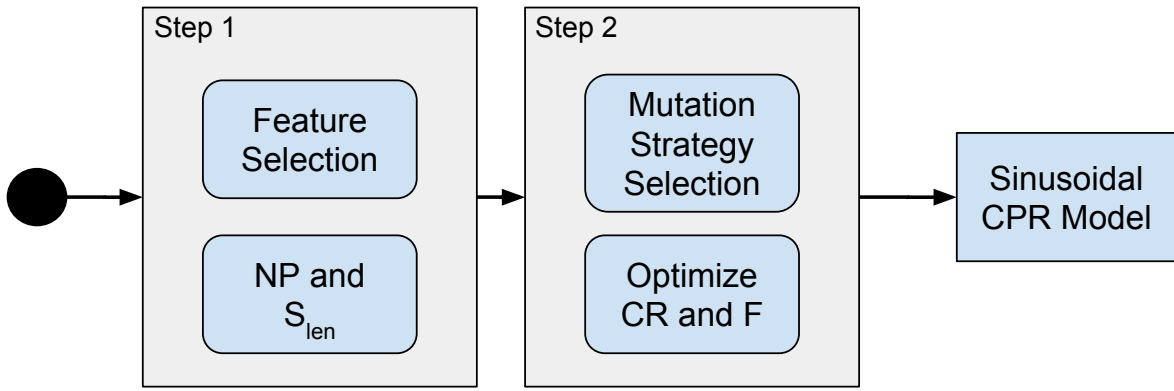


Figure 6: Study calculation steps overview.

### 2.4.1. Experimental setup

A Laerdal Resusci Anne Simulator mannequin was placed as reference-system on the floor. Within the mannequin, sensors measure the depth of thorax compression and decompression, the frequency of the compressions and the volume of ventilation, parameters which are visualized in real-time on a tablet and that can be downloaded as a summary of the training. The reference values can be obtained from the tablet after the CPR training process is finished.

A Kinect v2 sensor was placed at an approximate distance from the mannequin of 1.5 m and at the height of about 1 m. The person performing the CPR was placed on the other side of the mannequin facing the Kinect camera (see Figure 7) although no precise position or posture was enforced. The subject was asked to perform CPR compressions on the mannequin with standard CPR frequency and depth for about 90 seconds. The Kinect, as well as the Resusci Anne, were collecting data, which was synchronized manually after the recording using the RGB color image of the Kinect.

The participants were students and members of the University of Oldenburg. There were no inclusion or exclusion criteria. We conducted the experiment with 19 participants.

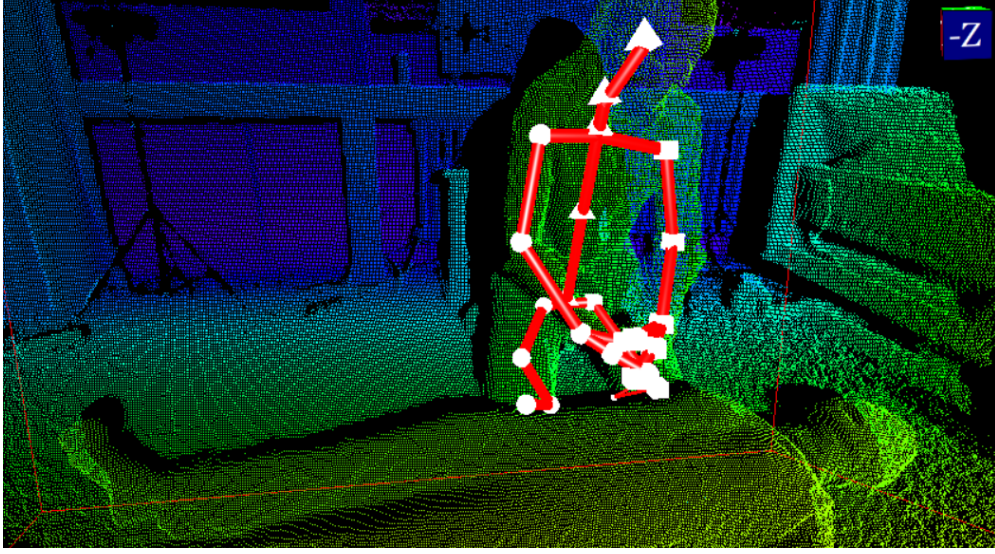


Figure 7: Voxel view of the 3D scene captured by the Kinect sensor with tracked skeleton as overview.

#### 2.4.2. Software and Parameter Settings

The R implementation of the DE algorithm (package DEoptim/2.2.4) [29, 30, 31] running on R/3.3.1 was used. We performed two slightly different evaluation steps that are described in this section.

*Optimize NP and Sample Set length.* For every trial we run the DE algorithm with the parameters specified in Table 1.

Table 1: DE parameter and parameter ranges for the first evaluation run.

Parameter	Strategy	CR	F	NP	$G_{max}$	$S_{len}$
Range	2	0.5	0.8	(25, 50, 75, 100, 150, 200)	200	(1,2,3,4,5) seconds

The used  $CR$ ,  $F$ , and strategy are the default parameters of the DE implementation. We vary the number of individuals ( $NP$ ) and the window length  $S_{len}$  used for the curve fitting ranging from 1 s to 5 s.

The sinus function  $y(t) = A \cdot \sin(2ft + \rho) + D$  within the cost function (see Equation 9) to be minimized here has four unknown variables ( $A, f, \rho, D$ ), but the solutions to the function can be limited due to the specifics of our problem and the nature of the sinusoid itself.  $A$  is the amplitude of the function. Valid values for  $A$  are limited by the observed and derived Y-axis coordinates by the Kinect (assuming Y-axis pointing upwards, so  $A \in (-2m, 2m)$ ). Same applies to  $D$ , the parameter that shifts the y value of the function in positive or negative direction, so we limit  $D \in (-2m, 2m)$  as well. The parameter  $\rho$  is the phase shift of the function, which is limited by the timestamps of our samples, so  $\rho \in (S_{start}, S_{end})$ . Finally,  $f$  is the frequency of the sinusoid, which we can limit to a reasonable range  $f \in (60\text{Hz}, 160\text{Hz})$ , so  $f \in (2\pi, \frac{16}{3}\pi)$ .

The Kinect samples with 30 Hz, so according to Nyquist-Shannon sampling theorem, the maximum reconstructible CPR frequency is 1800 cpm. The sample set length limits the minimum

reconstructible CPR frequency. A sample set of 5 s allows reconstruction of 12 cpm (or 6 cpm) when assuming a half period is enough to reconstruct the sinus curve).

*Optimization of Strategy, CR, and F.* Based on the results of the first run (see Section 3.1),  $NP = 50$  and  $S_{len} = 2s$  were chosen as fixed values. The mutation strategy as well as  $CR, F$  influence how fast the DE algorithm is converging towards a good solution, i.e. if the algorithm converges fast, it requires fewer generations/iterations and therefore runs faster. Thus, we investigated all possible combinations of  $CR, F$  within the given ranges  $[0, 1]$  respectively  $[0, 2]$ . The values used for this optimization step are summarized in Table 2. We use these parameters for the sinusoid fitting and the afterward comparison with the Resusci Anne reference values.

Table 2: DE parameter and parameter ranges for the second evaluation run.

Parameter	Strategy	CR	F	NP	$G_{max}$
Range	1, 2, 3, 4, 5, 6	$[0, 1]$	$[0, 2]$	50	30

The results of this DE constant optimization can be found in Figure 12.

### 2.5. Calculation of errors

The Resusci Anne mannequin records the CPR event based, i.e. each compression cycle (compression and decompression) is considered one event. For every event the start and end timestamps as well as the maximum compression depth and the current compression frequency are logged.

For every logged CPR event a sinusoidal model fitting was done using the last  $S_{len}$  Kinect samples beginning from the end timestamp of the event (see Equation 4). Then the difference between the currently fitted model frequency (after outlier filtering, see next paragraph) and depth prediction and the current event is calculated. For each trial the errors of every event are combined using median or mean.

*Outlier filtering.* The resulting frequency and depth prediction of the fitted models were filtered using interquartile range (IQR) of the predictions of the last  $5 \cdot S_{len}$  seconds to remove outliers.

$$p(t) = \begin{cases} p(t) & p(t) \in [Q_1 - 1.5 \cdot \text{IQR}, Q_3 + 1.5 \cdot \text{IQR}] \\ p(t-1) & \text{otherwise} \end{cases} \quad (10)$$

with  $p(t)$  the prediction at time  $t$ .

## 3. Results

In this section, we present the results of the evaluation and optimization of our approach. An overall of 12 participants (9 female, 3 male, age 21-47 (mean 30.25)) contributed 18 test runs. Two of the 12 participants reported that they are well-trained in CPR. We had to exclude the data of 7 of initially 19 participants due to recording errors of the storage system or malfunctions of the Kinect and Resusci Anne.

### 3.1. Fitting of MoCap Data to Sinusoid

First, it was examined how the different number of Kinect samples affect the accuracy of the sine fitting. Figures 9 and 8 show a comparison of median errors between model fitting and Resusci Anne data for the different limbs and different sample sizes that were used in the model. As can be seen in 8, the relative error for a sample length of one second is at 5 % deviation for the shoulders. It decreases at lengths of two seconds to about 2 %. Thus, we consider a sample length of two seconds and the shoulder limbs to be ideal for the model adaptation to the compression frequency. If longer data sets are used, the model will increasingly have difficulty adjusting to fast-changing frequencies.

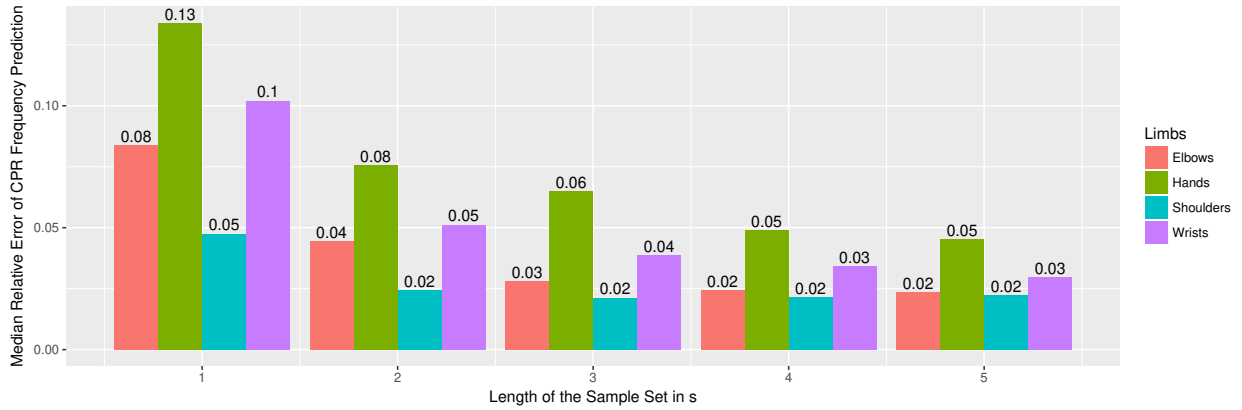


Figure 8: Comparison of the median CPR frequency error of elbows, hands, shoulders, and wrists for [1-5]s long sample sets. Results are the median errors combined for the runs with varying  $NP$ .

While the shoulders are suitable for model fitting for predicting the CPR frequency, they have deficits for adjusting the model regarding compression depth (see Figure 8). The hands or wrists are better suited here. The deviation is lowest for wrists at 31 % for a five second window, but barely higher for hands at 32 % for a two second window.

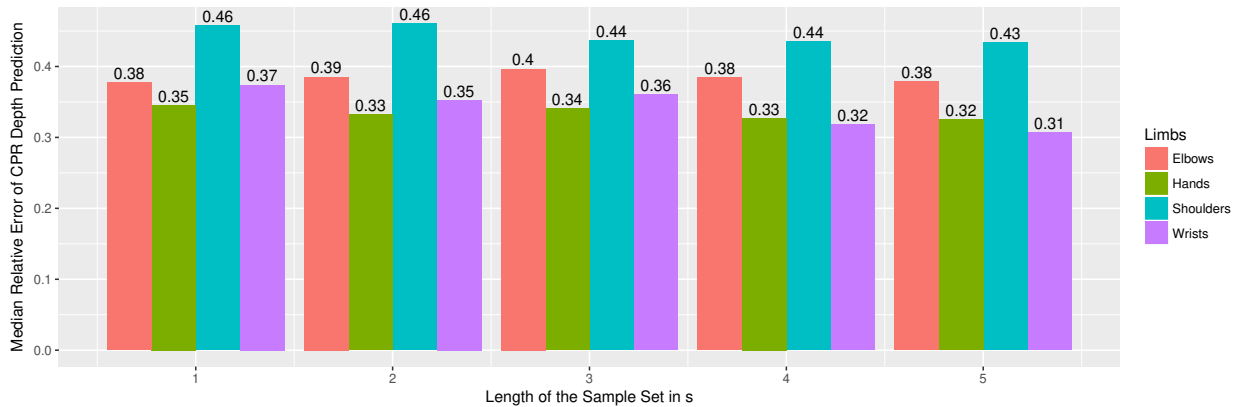


Figure 9: Comparison of the median CPR depth error of elbows, hands, shoulders, and wrists for [1-5]s windows

It was also investigated whether the size of the population used affects the accuracy of the model fitting. Figures 11 and 10 show a comparison of median errors between model fitting and Resusci Anne data for the different limbs and different population sizes that were used in the model. As can be seen from the figures, the population size has little to no impact on the model fitting. However, one can recognize here again that the shoulder joints are most suitable for the frequency prediction as well as the hands for the compression depth prediction.

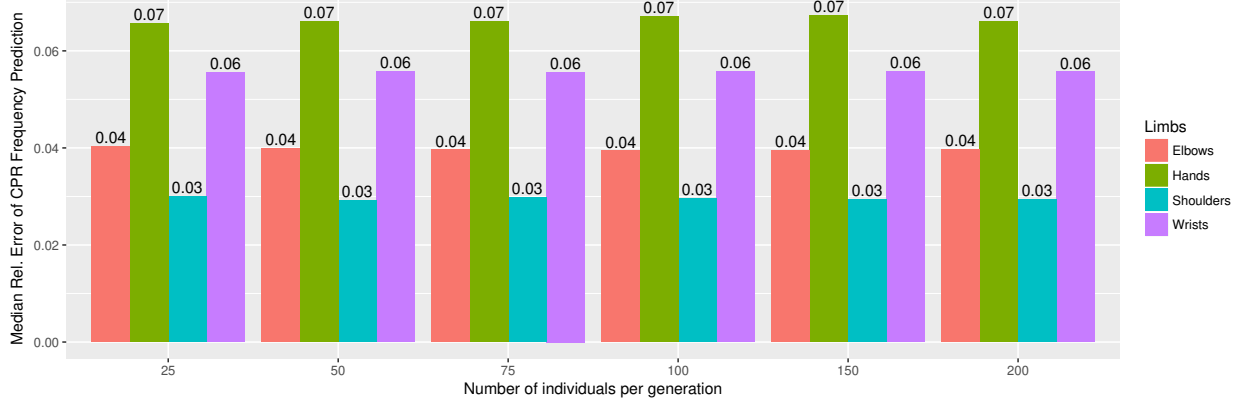


Figure 10: Comparison of the median CPR frequency error of elbows, hands, shoulders, and wrists for 25 to 200 DE individuals

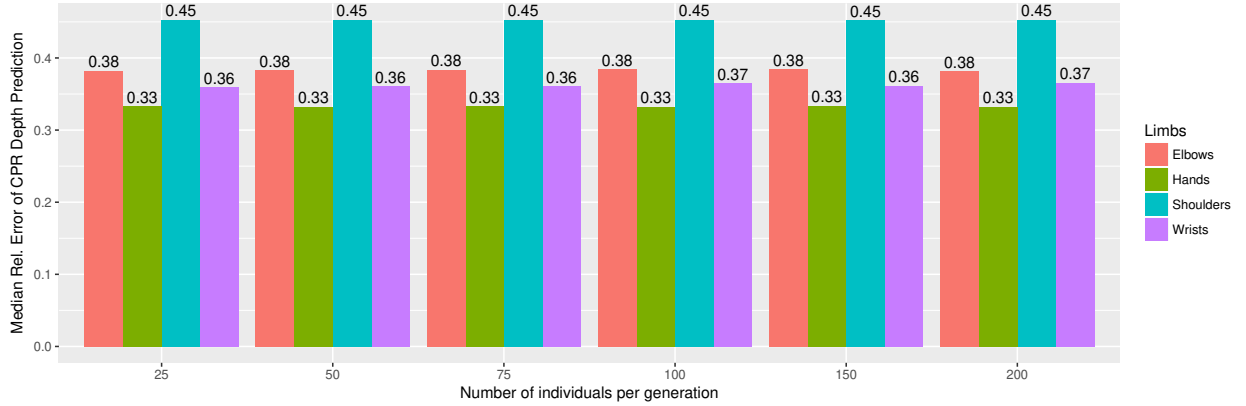


Figure 11: Comparison of the median CPR depth error of elbows, hands, shoulders, and wrists for 25 to 200 DE individuals

In summary, a population size of  $NP = 50$  and a sample length of  $S_{len} = 2s$  will have the most favorable effect on the fitting of the model. We take these parameters as defaults for further investigation. Table 3 shows the mean and median errors of this model summarized for all trials.

Table 3: Error results compared to Resusci Anne data for all trials using DE with ( $NP = 50, S_{len} = 2$ , shoulder) for frequency and ( $NP = 50, S_{len} = 5$ , hands) for depth.

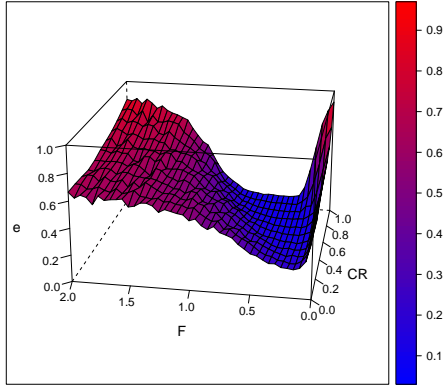
Rel. Freq. Error			Rel. Depth Error			Abs. Freq. Error in cpm			Abs. Depth Error in cm		
Median	Mean	SD	Median	Mean	SD	Median	Mean	SD	Median	Mean	SD
2.4 %	4.7 %	4.3 %	32.5 %	45.8 %	41.4 %	2.55	4.51	5.82	1.44	1.70	1.37

### 3.2. DE strategy and constant optimization

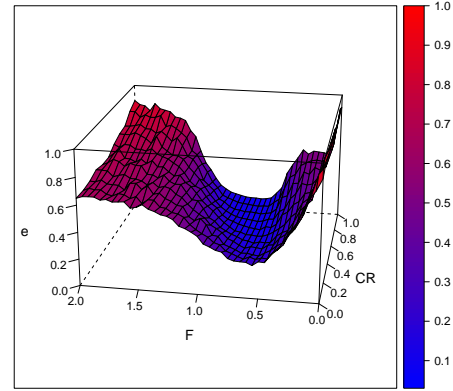
The mutation strategy as well as the constant parameters of the DE algorithm influence the convergence and thus the performance of the algorithm. Therefore we investigated the influence of DE constants  $F, CR$  and mutation strategy on the convergence towards a solution by calculating our standard fitting model ( $NP = 50, S_{len} = 2s$ ) with all variations of  $F$  and  $CR$  and six often used DE mutation strategies [31, 32, 33]. The cost function (see Equation 9) remained unchanged and the parameters were as of Table 2. We determined the minimal relative error and summarized the results in Table 4. Figure 12 visualizes the results for varying  $CR, F$  with the six different DE mutation strategies after 30 generations.

Table 4: Optimal  $CR, F$  for six DE mutation strategies ( $G_{max} = 30$ ).

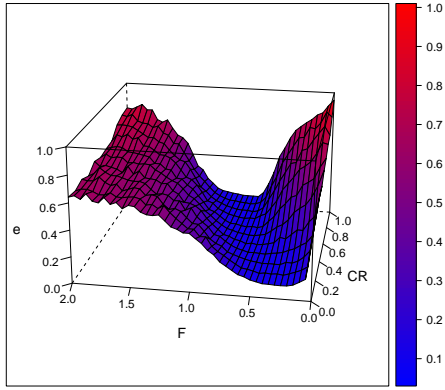
Mutation Strategy	CR	F	Min. Rel. Error
DE/rand/1/bin (classical strategy) [23]	0.9	0.35	9.68 %
DE/local-to-best/1/bin (default) [31]	0.9	0.75	9.22 %
DE/best/1/bin with jitter	0.9	0.75	9.35 %
DE/rand/1/bin with per-vector-dither	1.0	0.00	9.89 %
DE/rand/1/bin with per-generation-dither	1.0	0.00	10.04 %
DE/current-to-p-best/1	0.90	0.60	9.28 %



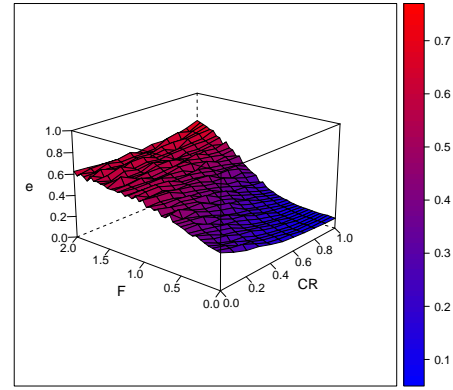
(a) Strategy DE/rand/1/bin



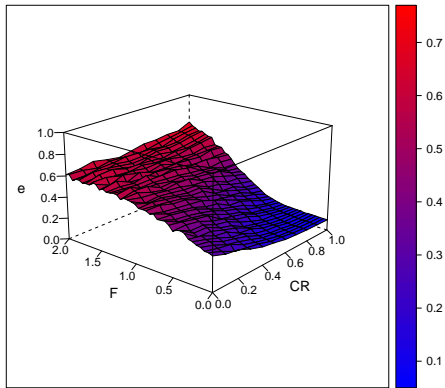
(b) Strategy DE/local-to-best/1/bin



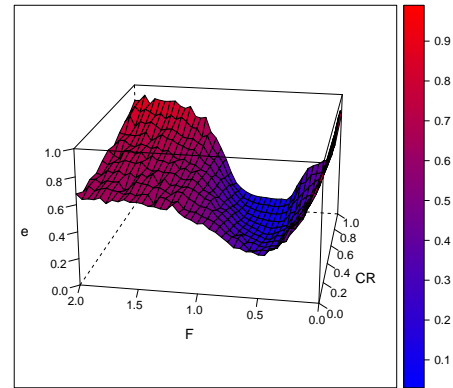
(c) DE/best/1/bin with jitter



(d) DE/rand/1/bin per-vector-dither



(e) DE/rand/1/bin per-gen.-dither



(f) DE/current-to-p-best/1

Figure 12: Influence of CR and F on relative error  $e$  for six different mutation strategies (30 generations). The smaller the error, the better the convergence.



## 4. Discussion

Accurate feedback on the frequency and depth of chest compressions is essential for CPR training or bystander CPR. Optical MoCap systems, in contrast to stationary mannequins, can observe the body position and movement of the trainee. Previous approaches using optical MoCap systems require additional markers on the trainee's hands or the training dummy [14], or require sophisticated image recognition algorithms to detect the trainee and pose [11]. Thus, systems for realistic environments are necessary.

The purpose of this study was to evaluate the accuracy of a sinusoidal model for deriving CPR quality parameters based on skeletal data from an optical MoCap system using the DE algorithm. It was evaluated which joint positions are best suited for fitting MoCap data to the model. To adjust the model for deriving the CPR frequency, the data of the shoulders result in the least error. In a previous examination [28], the fitting with the elbows had the least error, but the error of the shoulder was only marginally higher there. The shoulders are usually well visible from the sensors of the MoCap system, i.e. there are only a few mistakes in skeletal detection, which benefits the robust recognition of the CPR frequency. For the recognition of the compression depth, the shoulders are less suitable, the median relative error is comparatively high here with 43 %. Presumably, the bending of the arms when pressing on the rib cage falsifies the detection of the actual compression depth. Even very experienced rescuers bend their arms minimally while putting pressure on the thorax. The lower the flexion of the arms, the lower the fatigue of the rescuer. The position data of the hands is better for deriving the compression depth; here the median error is 30.5 % (1.3 cm) for the default model ( $NP = 50, S_{len} = 2s$ ). The error and the standard deviation are still comparatively high, one reason is certainly the high rate of false joint positions derived by the Kinect sensor, for example when a hand is hidden by the other one, which is the norm during CPR.

The accuracy with which our sinusoidal model can be used to derive the CPR frequency is in the range of other CPR training systems. We use a 2-second window to calculate the frequency with 2.4 % median error. This window size seems to be well suited for the frequency prediction, regardless of the technology used, as Ruiz de Gauna et al. [17] for example also use a 2-second window and report a median error of 5.9% for determining the CPR frequency with their IMU-based approach.

The accuracy of the compression depth model is comparatively low. With a median error of 32.5 % (1.44 cm), however, it is sufficient to make basic quality statements. An insufficient compression depth of, for example, 3 cm can be reliably distinguished from an adequate compression depth of 5.5 cm, so a basic feedback to the trainee is possible. One possible cause is the optical inaccuracy of the sensor used. Although the precision of the Kinect under optimal conditions is very high, under realistic conditions such as e.g. trainee is not front faced to the sensor, the accuracy drops quickly [34]. In this study, the subjects were deliberately not instructed on how to resuscitate the training dummy and how they should pose in front of the Kinect.

The approach of recording the motion data in a realistic setting shows the practicality of the model but does not exploit the maximum precision of the model.

In summary, our study shows that the positional data of shoulder and wrist joints that can be captured with optical MoCap systems can be used to fit a sinusoidal model. With this model,

robust quality parameters can be derived in realistic CPR training scenarios.

## 5. Conclusion

We presented a software system that uses motion data from an RGB-D (Kinect) sensor and the Differential Evolution (DE) optimization algorithm to dynamically fit sinusoidal curves to derive frequency and depth parameters for CPR training. We evaluated the approach with 18 trials of 12 different participants and tested the data of four different limb regions (hands, elbows, wrists, and shoulders) for their suitability to derive the parameters. Using the shoulder features of the Kinect skeleton, the results for the frequency determination show a mean variance of  $\pm 2.55$  cpm (2.4%) compared to the results of a Laerdal Resusci Mannequin (acting as the gold standard). We have also investigated which sample set length is the best tradeoff between adaptability to CPR frequency changes and precision. We found that a window size of  $S_{len} = 2s$  reduces the error between model prediction and Resusci Anne to a minimum.

We used different generation sizes for the DE optimization and found no significant precision differences whether a generation consists of 25, 50, 75, 100, 150 or 200 individuals. So  $NP = 50$  is recommended here.

We additionally compared six different DE mutation strategies and optimized the DE constants  $CR$  and  $F$  for each of this six strategies. We showed that both the classical `DE/rand/1/bin` and `DE/current-to-p-best/1` are converging fastest to a solution to our problem.

In addition to the frequency and compression depth, which are indeed the essential quality parameters for CPR, the flexion of the arms during the compression process could be considered as well. With the data of the Kinect, which can derive the positions of the shoulder, elbow, hands, and wrists, a measure of the flexion of the compression could be recorded. It remains to be investigated if the differences in compression depth between shoulder and hand models can be used to derive a degree of arm flexion. In the current method, the fitting of the model is continuously adjusted, but the DE algorithm assumes an entirely new fitting. It could still be investigated how the convergence and performance of the algorithm change when parts of the population (i.e., the possible solutions) are included, thus allowing a faster adaptation of the model. The difficulty here is also to react to extreme changes in the trainee's CPR and not to prematurely exclude parts of the solution space.

In conclusion, the approach described in this paper shows comparable and practical results that can contribute to novel CPR training devices that are suitable for use in both the lab, clinic, and field.

## Acknowledgements

We appreciate the support of Prof. Dr. Rainer Röhrig and Dr.-Ing. Myriam Lipprandt in the development of the initial research idea and in revision of the article.

This work was supported by the funding initiative Niedersächsisches Vorab of the Volkswagen Foundation and the Ministry of Science and Culture of Lower Saxony as a part of the Interdisciplinary Research Centre on Critical Systems Engineering for Socio-Technical Systems II.

The optimizations were performed at the HPC Cluster CARL, located at the Carl von Ossietzky University of Oldenburg (Germany) and funded by the DFG through its Major Research

Instrumentation Programme (INST 184/157-1 FUGG) and the Ministry of Science and Culture (MWK) of the Lower Saxony State.

## References

- [1] J. Berdowski, R. A. Berg, J. G. Tijssen, R. W. Koster, Global incidences of out-of-hospital cardiac arrest and survival rates: Systematic review of 67 prospective studies, *Resuscitation* 81 (11) (2010) 1479 – 1487. doi: <https://doi.org/10.1016/j.resuscitation.2010.08.006>.  
URL <http://www.sciencedirect.com/science/article/pii/S0300957210004326>
- [2] J.-T. Gräsner, J. Herlitz, R. W. Koster, F. Rosell-Ortiz, L. Stamatakis, L. Bossaert, Quality management in resuscitation towards a european cardiac arrest registry (eureca), *Resuscitation* 82 (8) (2011) 989 – 994. doi: <https://doi.org/10.1016/j.resuscitation.2011.02.047>.  
URL <http://www.sciencedirect.com/science/article/pii/S0300957211001961>
- [3] J.-T. Gräsner, L. Bossaert, Epidemiology and management of cardiac arrest: What registries are revealing, *Best Practice & Research Clinical Anaesthesiology* 27 (3) (2013) 293 – 306, saving 100,000 Lives Each Year in Europe. doi:<https://doi.org/10.1016/j.bpa.2013.07.008>.  
URL <http://www.sciencedirect.com/science/article/pii/S1521689613000530>
- [4] G. D. Perkins, A. J. Handley, R. W. Koster, M. Castrén, M. A. Smyth, T. Olasveengen, K. G. Monsieurs, V. Raffay, J. T. Gräsner, V. Wenzel, G. Ristagno, J. Soar, L. L. Bossaert, A. Caballero, P. Cassan, C. Granja, C. Sandroni, D. A. Zideman, J. P. Nolan, I. Maconochie, R. Greif, European Resuscitation Council Guidelines for Resuscitation 2015. Section 2. Adult basic life support and automated external defibrillation., *Resuscitation* 95 (2015) 81–99. arXiv:arXiv:1011.1669v3, doi:10.1016/j.resuscitation.2015.07.015.
- [5] V. J. De Maio, I. G. Stiell, G. A. Wells, D. W. Spaite, Optimal defibrillation response intervals for maximum out-of-hospital cardiac arrest survival rates, *Annals of emergency medicine* 42 (2) (2003) 242–250.
- [6] J. Soar, J. P. Nolan, B. W. Böttiger, G. D. Perkins, C. Lott, P. Carli, T. Pellis, C. Sandroni, M. B. Skrifvars, G. B. Smith, et al., European resuscitation council guidelines for resuscitation 2015, *Resuscitation* 95 (2015) 100–147.
- [7] R. F. Schmidt, F. Lang, F. Heckmann, *Physiologie des Menschen*, Springer Verlag, 2011. doi:10.1007/978-3-642-01651-6.  
URL <http://www.springer.com/us/book/9783642016509>
- [8] I. Hasselqvist-Ax, G. Riva, J. Herlitz, M. Rosenqvist, J. Hollenberg, P. Nordberg, M. Ringh, M. Jonsson, C. Axelsson, J. Lindqvist, T. Karlsson, L. Svensson, Early cardiopulmonary resuscitation in out-of-hospital cardiac arrest, *New England Journal of Medicine* 372 (24) (2015) 2307–2315, PMID: 26061835. arXiv:<https://doi.org/10.1056/NEJMoA1405796>, doi:10.1056/NEJMoA1405796.  
URL <https://doi.org/10.1056/NEJMoA1405796>
- [9] Y. Tian, S. Raghuraman, Y. Yang, X. Guo, B. Prabhakaran, 3d immersive cardiopulmonary resuscitation (cpr) trainer, in: *Proceedings of the 22nd ACM international conference on Multimedia*, ACM, 2014, pp. 749–750.
- [10] F. Semeraro, A. Frisoli, C. Loconsole, N. Mastronicola, F. Stroppa, G. Ristagno, A. Scapigliati, L. Marchetti, E. Cerchiari, Kids (learn how to) save lives in the school with the serious game Relive, *Resuscitation* 116 (2017) 27–32. doi:10.1016/j.resuscitation.2017.04.038.
- [11] C. Loconsole, A. Frisoli, F. Semeraro, F. Stroppa, N. Mastronicola, A. Filippeschi, L. Marchetti, Relive: a markerless assistant for cpr training, *IEEE Transactions on Human-Machine Systems* 46 (5) (2016) 755–760.
- [12] F. Semeraro, A. Frisoli, C. Loconsole, F. Bannò, G. Tammaro, G. Imbriaco, L. Marchetti, E. L. Cerchiari, Motion detection technology as a tool for cardiopulmonary resuscitation (CPR) quality training: A randomised crossover mannequin pilot study, *Resuscitation* 84 (4) (2013) 501–507. doi:10.1016/j.resuscitation.2012.12.006. URL <http://dx.doi.org/10.1016/j.resuscitation.2012.12.006>
- [13] E. Higashi, K. Fukagawa, R. Kasimura, Y. Kanamori, A. Minazuki, H. Hayashi, Development and evaluation of a corrective feedback system using augmented reality for the high-quality cardiopulmonary resuscitation training, in: *2017 IEEE International Conference on Systems, Man, and Cybernetics (SMC)*, 2017, pp. 716–721. doi:10.1109/SMC.2017.8122692.

- [14] J.-C. Wang, S.-H. Tsai, Y.-H. Chen, Y.-L. Chen, S.-J. Chu, W.-I. Liao, Kinect-based real-time audiovisual feedback device improves cardiopulmonary resuscitation quality of lower-body-weight rescuers, *The American Journal of Emergency Medicine*.
- [15] Z. Cao, T. Simon, S.-E. Wei, Y. Sheikh, Realtime multi-person 2d pose estimation using part affinity fields, in: *CVPR*, 2017.
- [16] V. Friedman, A zero crossing algorithm for the estimation of the frequency of a single sinusoid in white noise, *IEEE Transactions on Signal Processing* 42 (6) (1994) 1565–1569. doi:10.1109/78.286978.
- [17] S. Ruiz de Gauna, D. M. Gonzalez-Otero, J. Ruiz, J. K. Russell, Feedback on the rate and depth of chest compressions during cardiopulmonary resuscitation using only accelerometers, *PLOS ONE* 11 (3) (2016) 1–17. doi:10.1371/journal.pone.0150139.  
URL <https://doi.org/10.1371/journal.pone.0150139>
- [18] B. G. Quinn, Estimation of frequency, amplitude, and phase from the dft of a time series, *IEEE transactions on Signal Processing* 45 (3) (1997) 814–817.
- [19] A. Routray, A. K. Pradhan, K. P. Rao, A novel kalman filter for frequency estimation of distorted signals in power systems, *IEEE Transactions on Instrumentation and Measurement* 51 (3) (2002) 469–479. doi:10.1109/TIM.2002.1017717.
- [20] V. V. Terzija, Improved recursive newton-type algorithm for frequency and spectra estimation in power systems, *IEEE Transactions on Instrumentation and Measurement* 52 (5) (2003) 1654–1659. doi:10.1109/TIM.2003.817152.
- [21] P. K. Dash, B. R. Mishra, R. K. Jena, A. C. Liew, Estimation of power system frequency using adaptive notch filters, in: *Energy Management and Power Delivery*, 1998. Proceedings of EMPD '98. 1998 International Conference on, Vol. 1, 1998, pp. 143–148 vol.1. doi:10.1109/EMPD.1998.705491.
- [22] M. Sachdev, M. Giray, A least error squares technique for determining power system frequency, *IEEE Transactions on Power Apparatus and Systems* (2) (1985) 437–444.
- [23] R. Storn, K. Price, Differential Evolution A Simple and Efficient Heuristic for global Optimization over Continuous Spaces, *Journal of Global Optimization* 11 (4) (1997) 341–359. doi:10.1023/A:1008202821328.  
URL <http://dx.doi.org/10.1023/A:1008202821328>
- [24] K. V. Price, R. M. Storn, J. A. Lampinen, *Differential Evolution – A Practical Approach to Global Optimization*, Natural Computing, Springer, 2005.
- [25] K. Ishaque, Z. Salam, S. Mekhilef, A. Shamsudin, Parameter extraction of solar photovoltaic modules using penalty-based differential evolution, *Applied Energy* 99 (2012) 297–308. doi:10.1016/j.apenergy.2012.05.017.  
URL <http://dx.doi.org/10.1016/j.apenergy.2012.05.017>
- [26] H. Yousefi, H. Handroos, A. Soleymani, Application of Differential Evolution in system identification of a servo-hydraulic system with a flexible load, *Mechatronics* 18 (9) (2008) 513–528. doi:10.1016/j.mechatronics.2008.03.005.  
URL <http://dx.doi.org/10.1016/j.mechatronics.2008.03.005>
- [27] P. Pandunata, S. M. H. Shamsuddin, Differential Evolution optimization for Bezier curve fitting, *Proceedings - 2010 7th International Conference on Computer Graphics, Imaging and Visualization, CGIV 2010* (2010) 68–72doi:10.1109/CGIV.2010.18.
- [28] C. Lins, A. Klausen, S. Fudickar, S. Hellmers, M. Lipprandt, R. Röhrig, A. Hein, Determining cardiopulmonary resuscitation parameters with differential evolution optimization of sinusoidal curves, in: *Proceedings of the 11th International Joint Conference on Biomedical Engineering Systems and Technologies - Volume 5: AI4Health,, INSTICC, SciTePress, 2018*, pp. 665–670. doi:10.5220/0006732806650670.
- [29] B. Peterson, J. Ulrich, K. Boudt, Package 'DEoptim', *The R Journal*.
- [30] D. Ardia, K. Boudt, K. Mullen, B. Peterson, Large-Scale Portfolio Optimization with DEoptim (2014) 69–77.  
URL <http://www.universal-publishers.com/book.php?method=ISBN{&}book=1627345035>
- [31] D. Ardia, K. M. Mullen, B. G. Peterson, J. Ulrich, *DEoptim: Differential Evolution in R*, version 2.2-3 (2015).  
URL <http://CRAN.R-project.org/package=DEoptim>
- [32] R. Mallipeddi, P. Suganthan, Q. Pan, M. Tasgetiren, Differential evolution algorithm with ensemble of parameters and mutation strategies, *Applied Soft Computing* 11 (2) (2011) 1679 – 1696, the Impact of Soft Computing

- for the Progress of Artificial Intelligence. doi:<https://doi.org/10.1016/j.asoc.2010.04.024>.  
URL <http://www.sciencedirect.com/science/article/pii/S1568494610001043>
- [33] S. Das, P. N. Suganthan, Differential evolution: A survey of the state-of-the-art, *IEEE transactions on evolutionary computation* 15 (1) (2011) 4–31.
- [34] J. A. Diego-Mas, J. Alcaide-Marzal, Using kinect sensor in observational methods for assessing postures at work, *Applied Ergonomics* 45 (4) (2014) 976 – 985. doi:<https://doi.org/10.1016/j.apergo.2013.12.001>.  
URL <http://www.sciencedirect.com/science/article/pii/S0003687013002676>